0163-4984/87/1300–0103$02.20

Elemental Analysis Using Differential Absorption Techniques

H. RARBACK* AND F. CINOTTI

National Synchrotron Light Source, Brookhaven National Laboratory, Upton, NY 11973

and

C. JACOBSEN, J. M. KENNEY,† J. KIRZ, AND R. ROSSER

Department of Physics, SUNY, Stony Brook, NY 11794

ABSTRACT

X-ray differential absorption microanalysis is presented as a technique for trace element analysis of hydrated biological specimens of about 0.1–5 μm thickness. For the study of the light elements ($Z \leq 20$), the absorption technique minimizes the radiation dose and, thus, damage to such specimens when compared with X-ray fluorescence. A Scanning Transmission X-ray Microscope (SXTM) is described, which has been used to map the concentration of calcium in bone with better than 300 nm spatial resolution and a sensitivity to 5% calcium by weight. Future plans are briefly discussed that offer the hope of achieving 0.1% trace element sensitivity and 75 nm spatial resolution.

Index Entries: X-ray absorption microanalysis; X-ray microscopy; biological microanalysis; calcium distribution; bone.

INTRODUCTION

Progress in the biological sciences has been aided over the years by dramatic advances in techniques for mapping the elemental content of specimens. Electron probe microanalysis and Electron Energy Loss Spectroscopy (EELS) have provided both high trace element sensitivity and

*Author to whom all correspondence and reprint requests should be addressed.
†Present Address: King's College, Strand, London WC2 R2LS, England

high spatial resolution, but are well matched only to thin samples, and generally require a vacuum environment. The technique of proton-induced X-ray Emission (PIXE) offers even higher sensitivity to trace elements and the possibility of the specimen remaining in an atmospheric environment, but it cannot be used to resolve submicron structures. In addition, charged-particle probes typically involve exposing a specimen to a very high dose of damaging radiation (*1*).

For high spatial resolution, trace element analysis of relatively thick (1–10 μm), hydrated biological specimens, X-ray microprobes often prove to be the tools of choice. One still has a choice of tools, however: Hard X-rays can be used to stimulate X-ray fluorescence, whereas soft X-rays can detect specific low atomic number elements by means of differential absorption. In fact, X-ray fluorescence has met with considera-

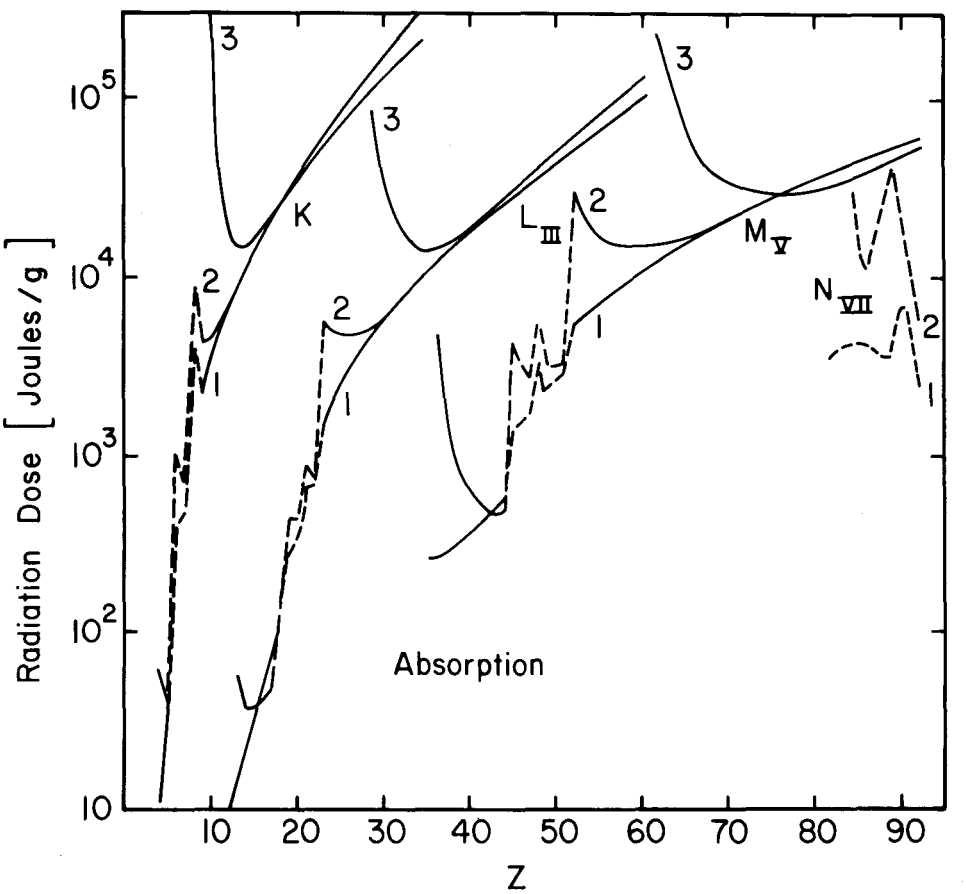

Fig. 1. Radiation dose required to establish the presence of 10^{-15} g of element Z in a $(1\text{-}\mu m)^2$ area of a specimen by differential absorption at the absorption edges indicated. Curves 1, 2, and 3 correspond to specimen thicknesses of 0.1, 1, and 10 μm, respectively. The specimen is assumed to be 50% protein and 50% water, by weight. The dashed portions of the curves correspond to energies near the C, N, or O absorption edges and are therefore sensitive to the nature of the specimen. From ref. (*4*).

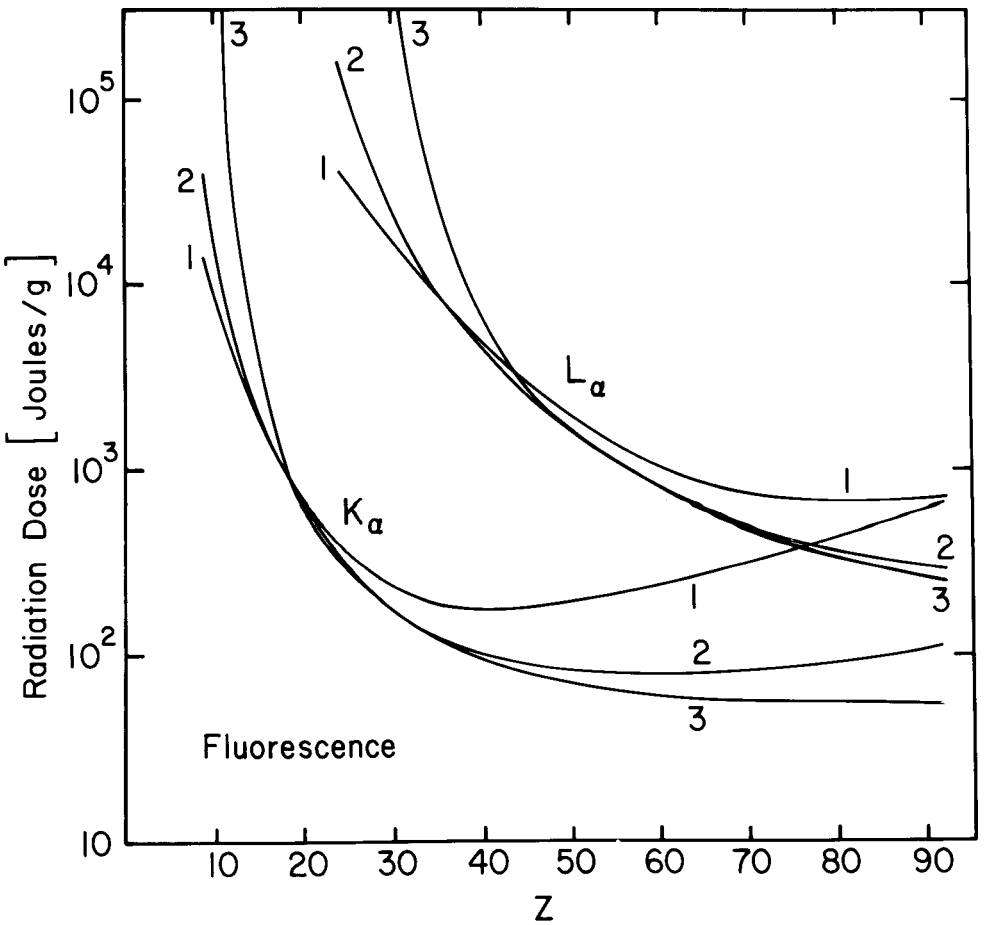

Fig. 2. Radiation dose required to establish the presence of 10^{-15} g of element Z in a $(1\text{-}\mu m)^2$ area of a specimen by X-ray fluorescence. From ref. (4).

ble success in the detection of trace elements (2), and a scanning fluorescence microscope was built that demonstrated 1-μm spatial resolution (3). There are fundamental reasons, however, why absorption is superior to fluorescence for trace analysis of low atomic number ($Z \leq 20$) elements in thick biological specimens. Primarily because of the low fluorescence yield of low Z elements, trace analysis of these elements involves a much higher radiation dose with the fluorescence technique than with absorption (4). This is clearly shown in Figs. 1 and 2, which plot the radiation dose necessary to detect the presence of 10^{-15} g of element Z in a $(1\ \mu m)^2$ area of 0.1, 1, and 1.0 μm thick, hydrated biological specimens by the two methods. (For a specimen density of 1 g/cm^3, this corresponds to a sensitivity of 1, 0.1, and 0.01%, respectively.) As can be seen, low Z elements can be detected with a much smaller dose using differential absorption rather than fluorescence when the specimen thickness is a few microns. Since most of the elements crucial to cell function are, in fact, within this range of Z, we feel that X-ray differential absorption will be-

come the method of choice for many biological studies using elemental analysis.

METHOD

With such considerations in mind, we have built a Scanning Transmission X-ray Microscope (STXM) that has attained a resolution of 0.2 μm with hydrated specimens (5), and have demonstrated its usefulness for elemental analysis by mapping the distribution of calcium in bone (6). The instrument operates on beam line U15 of the VUV ring at the National Synchrotron Light Source (NSLS), with a Toroidal Grating Monochromator (TGM) that allows one to use a bright, monochromatic beam of soft X-rays in the 1.5–4.5 nm wavelength region (7). A schematic diagram of the instrument is shown in Fig. 3. By demagnifying a pinhole source with a Fresnel zone plate (8), we produce an intense spot (200–300 nm in radius in the work reported here) through which we scan a specimen with a pair of piezoelectric transducers. This focused spot is brought out of the vacuum environment of the beam line through a 120-nm thick Si_3N_4 window, thus permitting the imaging of wet, living specimens in an atmospheric environment. Monitoring the incident flux with the CsI transmission photodiode and the transmitted flux with a gas-flow proportional counter provides an accurate method of measuring the X-ray absorption as a function of position in the specimen. The entire system is operated by an interactive software package implemented on a microcomputer, which allows the operator to easily control image formation as well as providing a real-time display of the image on a color monitor.

Differential absorption microanalysis makes use of the abrupt change in the soft X-ray attenuation of a specimen when the incident photon energy is changed from just below the absorption edge of some element in the sample to just above it. Since the change in the photon energies is only a few percent, the absorption of X-rays related to all other elements in the specimen will not change appreciably; consequently, any observed difference in the transmitted X-ray flux is related to the presence of the element under study. This phenomenon is easily exploited by the STXM because of its high efficiency of counting the X-rays transmitted through the specimen.

If we write the incident flux for each wavelength as $N_{Oh,Ol}$; the flux transmitted through the specimen as $N_{h,l}$; allow for a background X-ray flux of $B_{h,l}$; and have a mass absorption coefficient related to element Z of $\mu_{Zh,Zl}$, it can be shown that the mass thickness of element Z in the specimen, t_Z, is given by (9):

$$t_Z = \frac{\ln\left[\dfrac{(N_h - B_h)N_{Ol}}{(N_l - B_l)N_{Oh}}\right]}{(\mu_{Zl} - \mu_{Zh})} \qquad (1)$$

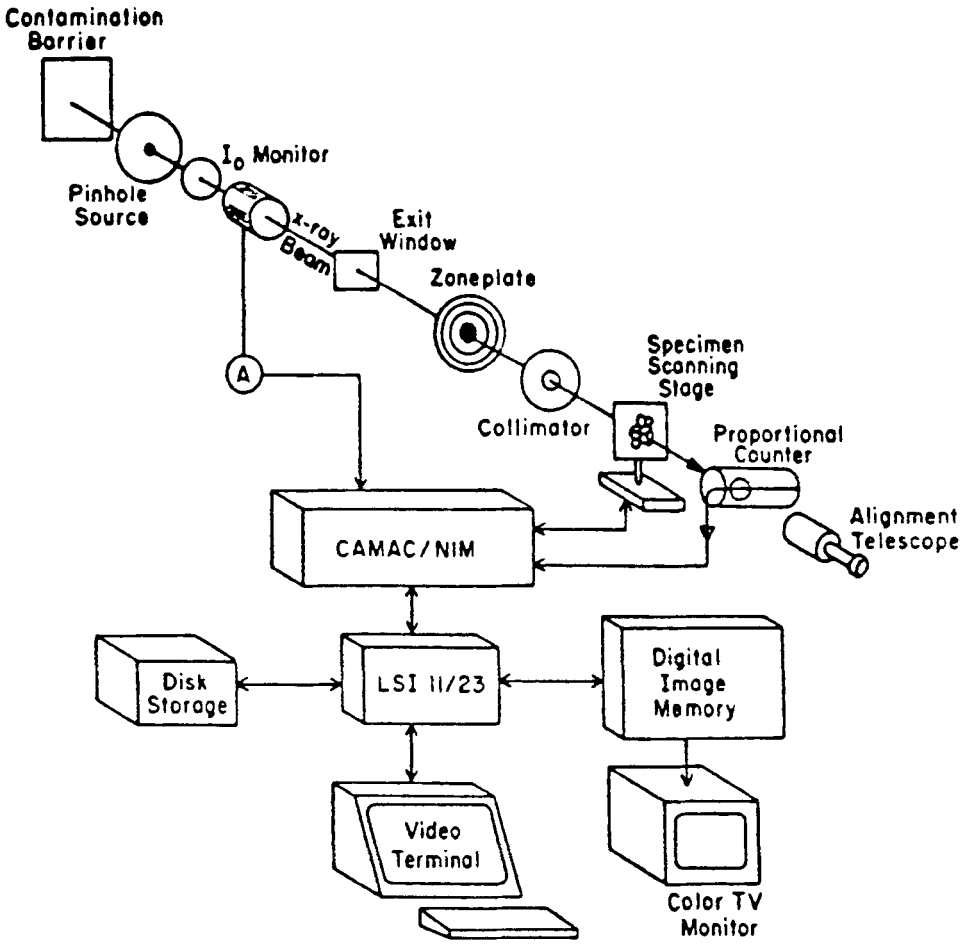

Fig. 3. Schematic of the Scanning Transmission X-ray Microscope.

The uncertainty in the measurement is:

$$\Delta t_Z = \frac{\left[\frac{N_h + \Delta B_h^2}{(N_h - B_h)^2} + \frac{N_l + \Delta B_l^2}{(N_l - B_l)^2} + \frac{1}{N_{Oh}} + \frac{1}{N_{Ol}} + [t_Z\,\Delta(\mu_{Zl} - \mu_{Zh})]^2\right]^{1/2}}{(\mu_{Zl} - \mu_{Zh})} \quad (2)$$

The background errors, $\Delta B_{h,l}$, arise from the fact that our detector is not position-sensitive, so it counts both the focused X-rays produced by the zone plate as well as nonfocused radiation. In the work reported here, the trace element sensitivity is limited by low incident flux $N_{Oh,Ol}$, not by background radiation.

RESULTS

We have examined sections of human skull tissue to test our ability to measure the distribution of calcium in bone. Small bone chips were

fixed in 3% glutaraldehyde in 0.15*M* phosphate buffer, dehydrated in ethanol, embedded in epoxy resin, and cut to 0.2-μm thickness, using a diamond knife. Sections were floated on water and heat-stretched prior to drying onto 2-mm diameter copper electron microscope grids. Optical micrographs taken of the specimens were used to determine potential regions of interest, and quick, coarse scans on the SXTM were used to select the features we examined in detail.

In the case of the calcium L_{III} absorption edge, the excitation of an

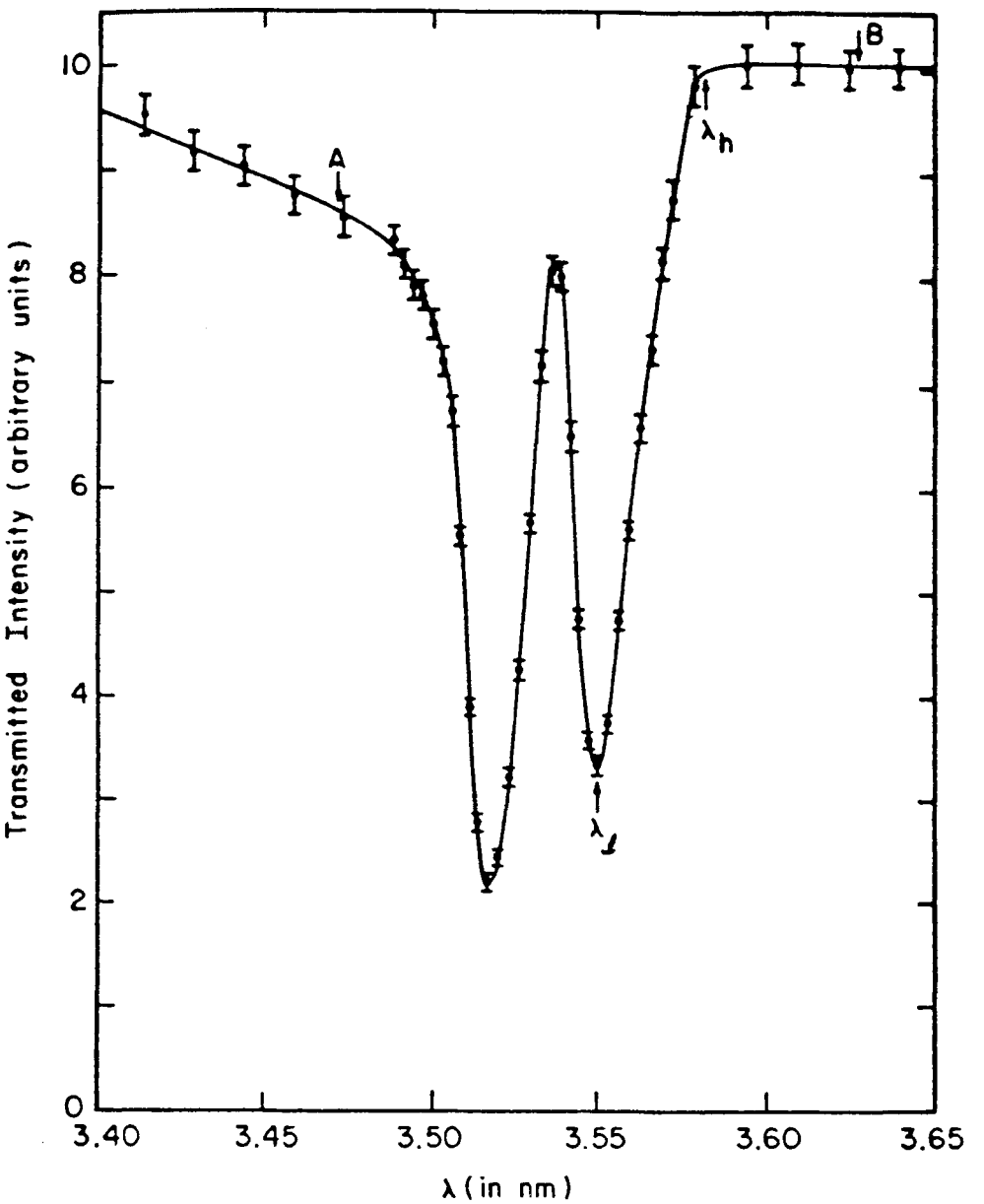

Fig. 4. Transmission spectrum of mineralized tissue in the human skull in the region of the calcium L_{II} and L_{III} absorption edges.

electron from the $2p$ state to the $3d$ state is complicated by wave function overlap effects (*10,11*), producing the observed calcium spectrum shown in Fig. 4. This feature turns out to be particularly advantageous for differential absorption microanalysis: the wavelengths λ_{II} and λ_I selected are quite close together, yet they exhibit drastically different absorption in calcium.

Figure 5 shows a series of X-ray micrographs of a 27 × 27 μm area of 200-nm thick human skull tissue. The images contain 140 × 140 pixels each, with a pixel size of 190 nm. The images include a grid bar in the upper left-hand corner, and a hole in the specimen in the lower right-hand corner, as verified by optical micrography. Figure 5(a) shows a transmission picture taken at λ_{II} of Fig. 4, whereas Fig. 5(b) was taken at λ_I. The difference between the two pictures is related almost entirely to calcium. Figure 5(c) is a map of calcium concentration in the specimen in terms of mass thicknesses ranging from 0 to 10 μg/cm^2. (The overall specimen mass thickness was estimated to be 40 μg/cm^2.)

The ability of the SXTM to resolve the various calcium concentrations is indicated in Fig. 6, which plots the relative uncertainty in t_Z measurements. This figure indicates that the error in t_Z is 0.5–1 μg/cm^2 for $t_Z \leq 6$ μg/cm^2, and becomes larger for higher concentrations. At the 5 SD level, our instrument is currently limited to detecting about 2 μg/cm^2, or roughly 5% calcium by mass. The spatial resolution is shown in Fig. 7, which is a histogram of calcium mass thickness for a scan line across the bottom of Fig. 5(c). The histogram includes many jumps from no calcium to heavy calcium concentrations over a one or two pixel distance, showing a spatial resolution of roughly 300 nm.

DISCUSSION

We are in the process of improving our instrument's elemental sensitivity and spatial resolution. Our current sensitivity to a calcium concentration of no less than 5% is limited primarily by the flux of our synchrotron radiation source. We are eagerly awaiting the commissioning of an undulator-based beam line (X1) on the X-ray ring of the NSLS, which should provide us with a 10^4 increase in our focused soft X-ray flux. At that point, our current X-ray background levels would limit us to a minimum detectable calcium concentration of about 0.1%, and it may become possible to detect a calcium concentration of roughly 100 ppm. With improved zone plates, we also expect to improve our probe radius (and thus spatial resolution) to 75 nm or better.

SUMMARY

Although the sensitivity of the SXTM to trace elements does not approach that of other microprobes now available, we feel that it holds

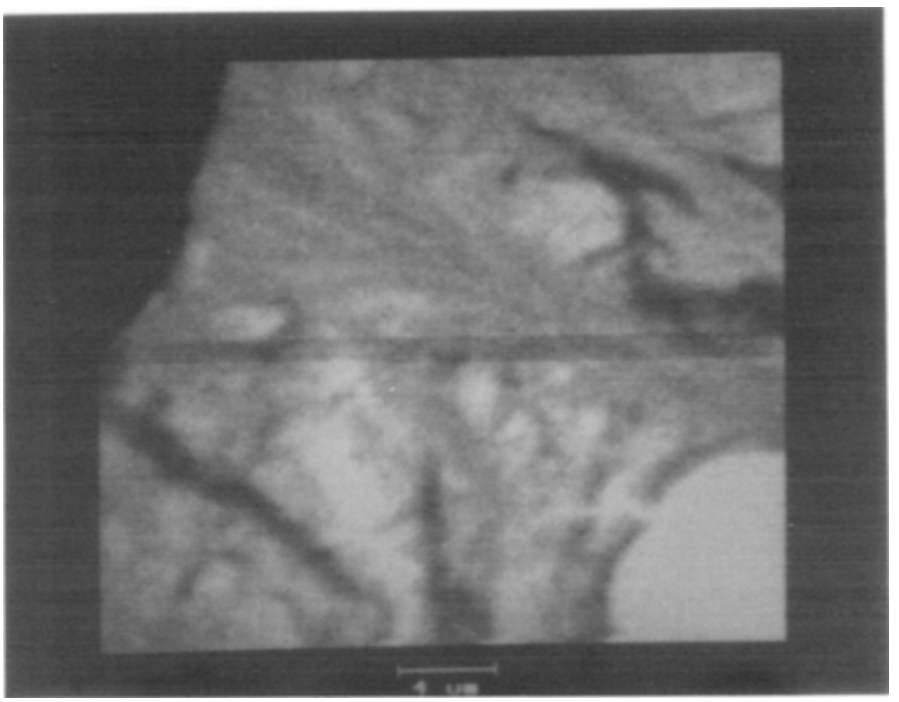

5a

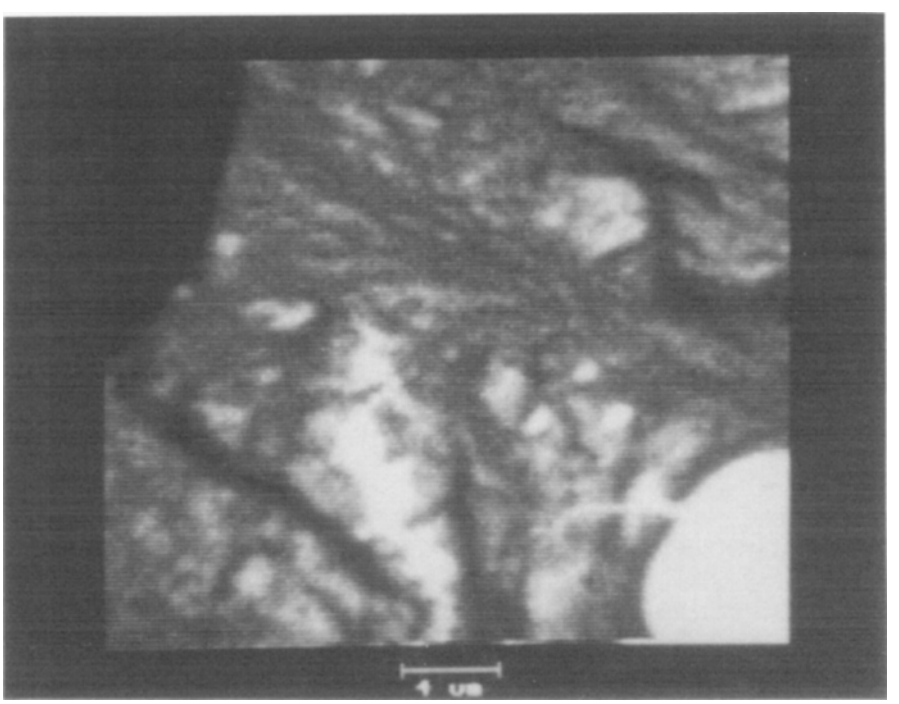

5b

Fig. 5. A series of X-ray micrographs of a (27-μm)^2 area of 200 nm thick human skull tissue. (a) Transmission picture taken at λ_{II} of Fig. 4. (b) Transmission picture taken at λ_I of Fig. 4. (c) Calcium map of the specimen, with a gray scale that runs from 0 to 10 μg/cm^2.

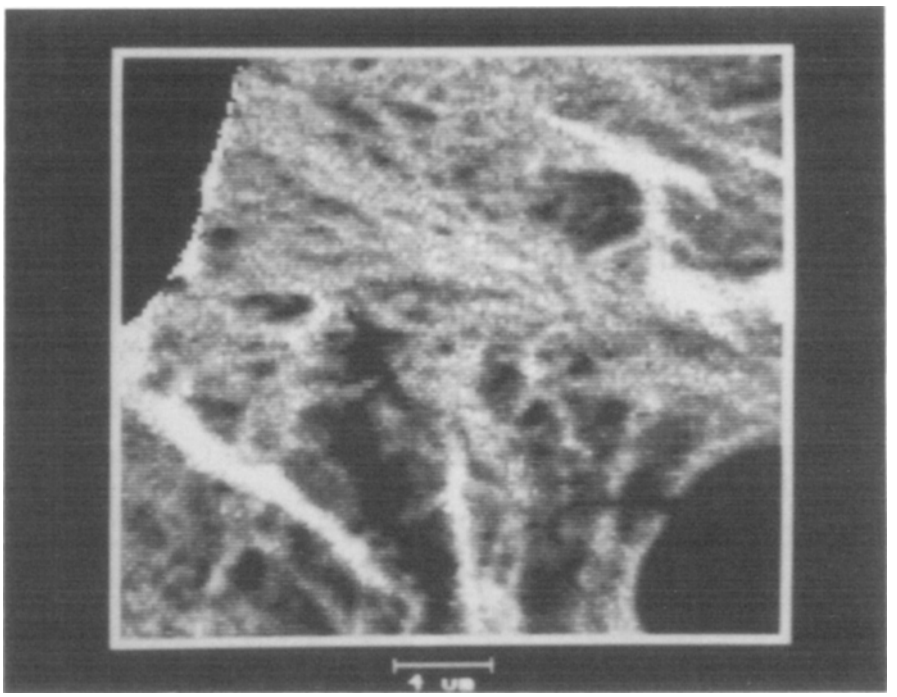

5c

much potential. As the sensitivity improves, the advantages of high spatial resolution and the ability to image wet, initially living specimens will become important factors to biologists interested in microanalysis. X-ray fluorescence will remain the technique of choice for high Z elements in such specimens, for it imparts a lower radiation dose and allows one to collect information on several elements at one time. When $Z \leqslant 20$ elements are to be mapped, however, X-ray differential absorption microanalysis is the most appropriate method.

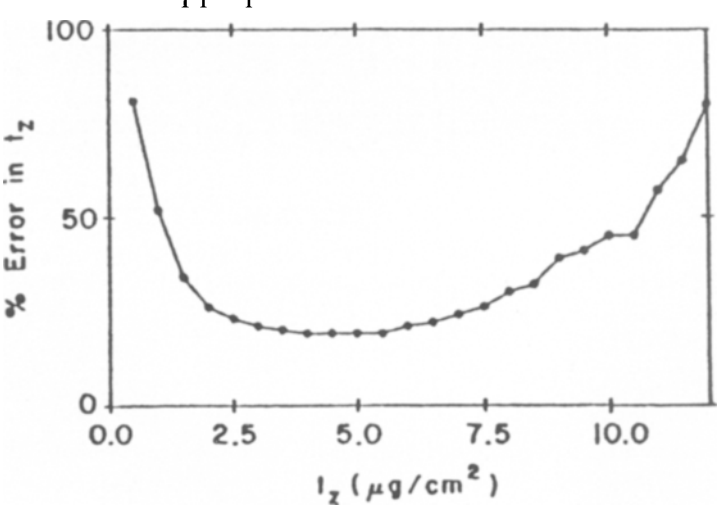

Fig. 6. Percent error in t_Z versus calcium mass thickness t_Z for the micrograph in Fig. 5(c).

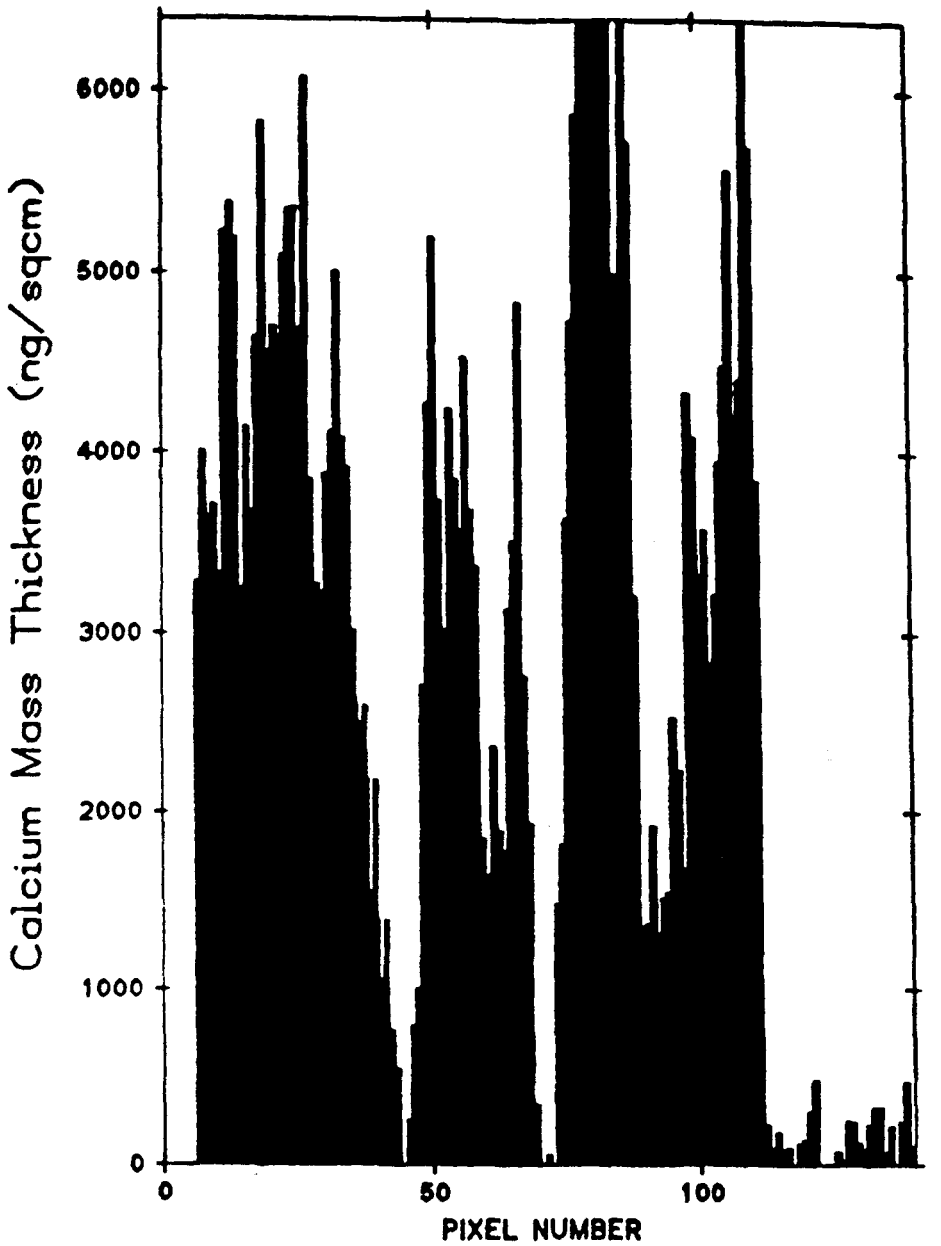

Fig. 7. Histogram of calcium mass thickness versus horizontal pixel location along a scan line near the bottom of Fig. 5(c).

ACKNOWLEDGMENTS

We are grateful to our colleagues at Brookhaven, Stony Brook, and IBM who made this work possible. In particular, we thank W. Thomlinson, G. Schidlowsky, R, Feder, and D. Sayre for their important contributions. This work was supported in part by the Department of En-

ergy under contract DEAC0276CH00016 (Brookhaven) and by the National Science Foundation under grant DMB-8410587 (Stony Brook). This work based in part on a dissertation submitted by J.M.K. to the Department of Physics, SUNY at Stony Brook, 1985.

REFERENCES

1. J. Kirz, in *Scanning Electron Microscopy* II, SEM, Chicago, IL, 1980, pp. 239–249.
2. C. J. Sparks, in *Synchrotron Radiation Research*, S. Doniach and H. Winick, eds., Plenum, New York, NY, 1980, pp. 459–509.
3. P. Horowitz and J. A. Howell, *Science* **178,** 608 (1972).
4. J. Kirz, in *Ultrasoft X-Ray Microscopy: Its Application to Biological and Physical Sciences*, D. Parsons, ed., *Ann. New York Acad. Sci.* **342,** 273 (1980).
5. H. Rarback, J. M. Kenney, J. Kirz, M. R. Howells, P. Chang, P. J. Coane, R. Feder, P. J. Houzego, D. P. Kern, and D. Sayre, in *X-Ray Microscopy*, G. Schmahl and D. Rudolf, eds., Springer-Verlag, Berlin, 1984, pp. 203–215.
6. J. M. Kenney, C. Jacobsen, J. Kirz, H. Rarback, F. Cinotti, W. Thomlinson, R. Rosser, and G. Schidlovsky, *J. Microscopy*, **137,** 321 (1985).
7. J. M. Kenney, J. Kirz, H. Rarback, M. R. Howells, P. Chang, P. J. Coane, R. Feder, P. J. Houzego, D. P. Kern, and D. Sayre, *Nucl. Inst. Meth.* **222,** 37 (1984).
8. The zone plate used for this work was fabricated at the IBM T. J. Watson Research Center, Yorktown Heights, NY. For details, *see* D. Kern *et al.*, *J. Vac. Sci. Technol.* B **1,** 1096 (1983).
9. J. M. Kenney, *Elemental Analysis using a Scanning Transmission X-ray Microscope: Mapping Calcium Concentration in Human Bone*, Ph. D Dissertation, SUNY at Stony Brook, NY (1985).
10. M. W. D. Mansfield, *Proc. Royal Soc. London* **A348,** 143 (1976).
11. J. P. Connerade, *Contemp. Phys.* **19,** 415 (1978).